ARTICLE

JOURNAL`S UNIVERSITY OF BABYLON FOR ENGINEERING SCIENCES (JUBES)
مـــجلـة جـــامعة بـــابـل للعلـــوم الهندسية

Vol. 33, No.6. \ 2025 ISSN: 2616 - 9916

Photocatalytic Degradation of Basic Fuchsin From Aqueous Solution Using Zinc Oxide / Metakaolin Composite

Ebtehaj Ahmed[1], Rasha A.Al-Husseiny[2]

[1,2] *Water Resources Engineering Department , College of Engineering, Al-Qasim Green University, 51013 Babylon, Iraq*

Corresponding Author Email [1]: ebtehijahmed@wrec.uoqasim.edu.iq

Author Email[2]: rasha83@wrec.uoqasim.edu.iq

Received:	24/11/2025	Accepted:	28/12//2025	Published:	31/12/2025

Abstract:

Hazardous organic pollutants are a common environmental problem, as they do not readily decompose in the environment, leading to their accumulation and a negative impact on ecosystems and human health. Therefore, finding effective and sustainable ways to dispose of them is crucial for preserving the environment and mitigating the health risks associated with them. Consequently, this work demonstrated a cost-effective, environmentally friendly, and straightforward technique for creating a zinc oxide nanocomposite using potato peels (PP).This nanocomposite, known as ZnO-PP,was synthesized and then combined with metakaolin yo from a composite with the prepared material to form a composite designed to facilitate an advanced oxidation process (AOP) for the removal of basic fuchsin (BF) from aqueous media.Comprehensive characterization of the synthesized composites was performed using several analytical instruments, including Fourier Transform Infrared Spectroscopy (FTIR), X-ray Diffraction (XRD), Field-Emission Scanning Electron Microscopy (FESEM),and Brunauer–Emmett–Teller (BET) surface area analysis. The BET results indicated specific surface areas of 2.95 m^2/g for raw potato peels (PP), 15.985 m^2/g for ZnO-PP, 28.251 m^2/g for ZnO-MK composite. Under optimal conditions, namely a ZnO-MK dosage of 0.15 g per 100 mL solution, an initial BF concentration of 10 mg/L, a contact time of 120 minutes, and pH 7 the composite achieved a maximum dye removal efficiency of 96%. Kinetic evaluation revealed that the degradation of BF conformed to a pseudo-first-order rate model, with a coefficient of determination (R^2) of 0.9526.

Keywords: Basic fuchsin (BF); Green synthesis; Photocatalytic; Potato peels (PP); Zinc oxide (ZnO).

1. Introduction:

Water pollution is becoming a major global environmental problem due to the discharge of contaminants from various anthropogenic activities, especially industrial processes. The contaminated water may expose consumers to illness or death in some cases, and aquatic life becomes unsafe for sustaining healthy life[1]. The presence of chemical, physical, or biological species that alter water quality and have the potential to impact ecosystems negatively is referred to as water pollution.This pollution harms drinking water, groundwater, and surface water, resulting in significant health repercussions.Many industries, such as paper, leather, cosmetics,

food, and textile, use dyes and pigments in their manufacturing processes to colour its products[2].

The textile industry is classified as the first industry to use high amounts of dyes in colouring their products, so their effluents are a common source of water pollution and are responsible for intensifying environmental problems[3].

Basic Fuchsin, commonly known as Basic Violet 14, is a cationic dye that has been designated as a possible carcinogen in numerous nations because of its poisonous and carcinogenic qualities. It can also stain collagen, muscles, mitochondria, and tuberculosis bacteria. It contains anesthetic, antibacterial, and fungicidal effects. Direct contact with the dye can cause substantial irritation to the eyes and skin[4].

Many technologies have been employed, including chemical precipitation, solvent extraction, adsorption, sedimentation, electrochemical processes, and traditional biological processes. Unfortunately, these technologies require precise temperature and pressure control, are not cost-effective, and have lengthy processing times[5].The advanced oxidation process(AOP) has shown promise in removing contaminants from aquatic environments and is a reliable, economical, and efficient solution[6].By using various catalysts, homogeneous and heterogeneous photocatalysis have demonstrated promise among the many AOP approaches in degrading a variety of contaminants, which utilize multiple catalyst types[7]. Advanced oxidation processes (AOPs) are increasingly recognized as cost-efficient and environmentally benign options for wastewater remediation (Al-Husseiny et al., 2023). Owing to their superior performance, minimal toxicity, reduced energy requirements, and proven capacity to treat municipal effluents, nanoscale semiconductor photocatalysts—such as TiO_2, ZnO, and Fe_2O_3—have become a focal point of contemporary research [8]. Among these, zinc oxide (ZnO), a member of the II–VI semiconductor family, is classified as a wide-bandgap material. Under irradiation with photons exceeding its bandgap energy, ZnO activates photocatalytic degradation of organic contaminants. This process generates electron–hole pairs, whereby electrons are promoted from the valence band to the conduction band, leaving behind positively charged holes that collectively drive photodegradation reactions [9]. A very eco-friendly method for creating ZnONPs is green synthesis[10]. Zinc oxide is produced from zinc ores through complex processes. However, growing interest is being placed in more sustainable methods for producing zinc oxide from waste materials, such as agricultural by-products[11]. One such potential source includes potato peels, a common food industry waste material. Potato peels contain natural biomolecules like starch, polyphenols, and sugars that act as reducing and stabilizing agents in nanoparticle synthesis. These biomolecules reduce the zinc salts to zinc oxide nanoparticles without the use of toxic chemicals[12].

Metakaolin is activated kaolin clay, which is prepared by heating kaolin to a specific temperature(about 500-800°C). It develops a higher surface area and porosity as a consequence of this and acts as a good adsorbent for various pollutants,including dyes. The adsorptive capacity of metakaolin can be further enhanced by modifying its surface properties [13], [14] .In various industrial sectors, especially in construction and material science, The ZnO-MK composite are gaining significant attention ZnO-MK . When mixed, ZnO-MK form a composite material based on adsorption and photocatalytic degradation. The composite degrades the dyes through photocatalysis when exposed to UV light Both ZnO-MK

are cheap, so the composite offers a low-cost wastewater treatment option [15]. The aim of this study was a simple and green synthesis approach of a composite ZnO-MK using the waste product from potato peels as a reducing and capping agent for the removal of organic pollutant (acid fuchsin) through the photocatalytic activity of the ZnO and ZnO-MK structures. Through the application of various spectroscopic and microscopy techniques, the ZnO and ZnO-MK nanostructures were characterized and assessed. XRD, FESEM, BET, and FTIR using the Barrentt-Joyner-Halenda method were used to analyze the produced materials.

2. Materials and Methods:

2.1 Materials:

A diverse range of materials was employed throughout the experimental procedures, and all reagents were of analytical-grade purity to ensure reliability and reproducibility of results. The dye (BF) was used as a contaminant model supplied Sigma-Aldrich (a part of Merck Group, Germany). Zinc nitrate hex hydrate was used. Kaolin ,Hydrochloric acid (HCl) ,and sodium hydroxide (NaOH) were used.

2.2.1 Preparation of Nanocomposite (ZnO-PP) :

To ensure the removal of residual fine particulates, the collected potato peels obtained from a local market were repeatedly washed with clean water. Subsequently, the material was subjected to ambient air-drying for approximately three days until complete moisture loss was achieved. The dried peels were then milled into a uniform powder and stored in a sealed, airtight container. Potato peel has been used as a fuel in the combustion route to produce ZnO-PCs. 3g of zinc nitrate hexahydrate $Zn(NO_3)_2 \cdot 6H_2O$, 99.999%, Sigma-Aldrich, Germany) was dissolved in 10 mL of DI water, then 1g of peels was gently added to it while stirring for 30 minutes. The mixture was transferred to a borosil glass container and kept in a preheated muffle furnace at 500 °C for 10 minutes of combustion. During this process, a large amount of heat and gases were evolved continuously; resulting white-colored voluminous porous nanopowder was obtained,as illustrated in the fig.(1)The processes of the synthesis of (ZnO-PP).

Fig. (1): ZnO-PP preparation steps.

Vol. 33, No.6. \ 2025 ISSN: 2616 - 9916

2.2.2 Synthesis of a zinc oxide/metakaolin(ZnO-Mk)composite:

High-reactivity metakaolin was produced through the controlled calcination of pure kaolin clay. A specialized calcination furnace was used to perform the thermal treatment, where the samples were heated at a controlled rate of 5°C/min. Upon reaching the target temperature of 750°C, the samples were held at this temperature for 3 hours. This precise process ensures the near-complete dehydroxylation, transforming the crystalline structure of kaolinite into the amorphous metakaolin phase ($Al_2Si_2O_7$). In this work, 1.8 g of ZnO was added to 10 ml of distilled water,and stir for 10 to 15 min. then, 1.2 g of metakaolin was added, and stir continuously to avoid clumping. Next, the mixture was drying in an oven at 105-120°C. After drying, the resulting material was ground and then calcined for 3 h at 500°C. fig. (2) depicts the stages of the synthesis of (ZnO-MK).

Fig.(2) Steps of synthesis of (ZnO-MK).

2.3 Parameters affecting the photocatalytic process.

This study conducted trials utilizing variable parameters in a batch system, as illustrated in Table (1):

Table (1): Batch system analysis of experimental parameters.

Parameters Range	Ranges
pH	(2-10)
Dosage g/100ml	(0.025-0.25)
Initial concentration (ppm(mg/L))	(10-50)
Contact time (min)	(30-180)

Vol. 33, No.6. \ 2025 ISSN: 2616 - 9916

The efficiency of BF removal, represented as R (%), was calculated using equation 1 [16],

$$\textbf{Degradation efficiency } \% = \frac{Co - Ct}{Co} * 100\% \quad (1)$$

Where C_0 represents the initial dye concentration, and C_t corresponds to the basic fuchsin concentration at a given time during the reaction.

3. Results and discussions:

3.1. Results of characterization:

3.1.1 Brunauer–Emmett–Teller (BET) and Barrentt-Joyner-Halenda (BJH) Analysis:

The specific surface areas of the adsorbents were quantified using the Brunauer–Emmett–Teller (BET) method, while the pore characteristics were evaluated via the Barrett–Joyner–Halenda (BJH) technique. The BET analysis revealed that the surface areas of potato peels (PP), ZnO-PP, and ZnO-MK prior to dye adsorption were 2.95, 15.985, and 28.251 m^2/g, respectively. Moving to the Total Pore Volume, it follows the same upward trend. The pore volume increases from a modest value of 0.0135 cm^3/g in the raw material (PP) to 0.1729 cm^3/g in ZnO-PP, and reaches its maximum value in the ZnO-MK composite at 0.1823 cm^3/g. This steady increase confirms that the modification processes were not limited to the external surface but also led to the creation of an extensive network of internal voids and pores. Correspondingly, the average pore diameters of PP, ZnO-PP, and ZnO-MK before adsorption were determined to be 7.98, 5.32, and 5.32 nm, respectively, this reduction, concurrent with the immense increase in surface area and pore volume, strongly suggests that the enhancement mechanism relies on the generation of a large number of smaller pores rather than the widening of existing ones. The larger surface area and pore volume provide a greater number of active sites on the surface for further adsorption of reactive molecules, which results in a photocatalytic reaction with higher efficiency[17].

3.1.2 X-Ray Diffraction (XRD) analysis:

The crystallinity, phase composition, and crystal particle size of the synthesized materials were investigated using X-ray diffraction (XRD) analysis. Fig.3(a–d) illustrates the crystalline structures of ZnO-PP, metakaolin (MK), ZnO-MK before removal, and ZnO-MK after BF removal. For ZnO-PP, diffraction peaks were observed at 2θ values of 32°, 35°, 38°, 47°, 56°, 62°, 67°, and 70°, as shown in Fig(3-a). The presence of sharp and well-defined peaks indicates a highly crystalline structure, which corresponds closely with JCPDS card no. 036-1451 for ZnO[18]. The XRD pattern of MK, depicted in Fig(3-b), displays a prominent peak around 27°, suggesting the dominance of a major crystalline phase. Additionally, broader secondary peaks are evident at approximately 21°, 36°, 50°, 60°, and 68°, consistent with JCPDS card no. 046-1045 for metakaolin[19]. Figure (c) shows sharp diffraction peaks consistent with the hexagonal wurzet structure of zinc oxide (ZnO), confirming its high crystallinity, while metakaolin acts as an amorphous substrate. In Fig (3-d), after dye adsorption, the peak positions remain stable, indicating the structural stability of the compound. The marked decrease in peak intensity is attributed to the coating of the crystal surface with dye molecules, demonstrating that

the removal occurred via a surface adsorption mechanism without altering the material's fundamental structure.

Accordingly, the crystallite diameter (D) was determined utilizing Scherrer's equation,

$$D = K\lambda / \beta \cos\theta \qquad (2)$$

Where the symbol "K" stands for the Debye Scherrer constant, λ denotes the X-ray wavelength, β\betaβ corresponds to the full width at half maximum (FWHM) of the diffraction peaks, and θ\thetaθ is the Bragg diffraction angle[20]. Using the XRD data, the morphological analysis of the materials revealed a ZnO particle size of 21.8 nm. This was consistent with the enhanced removal efficiency of BF by the (ZnO-MK) composite.

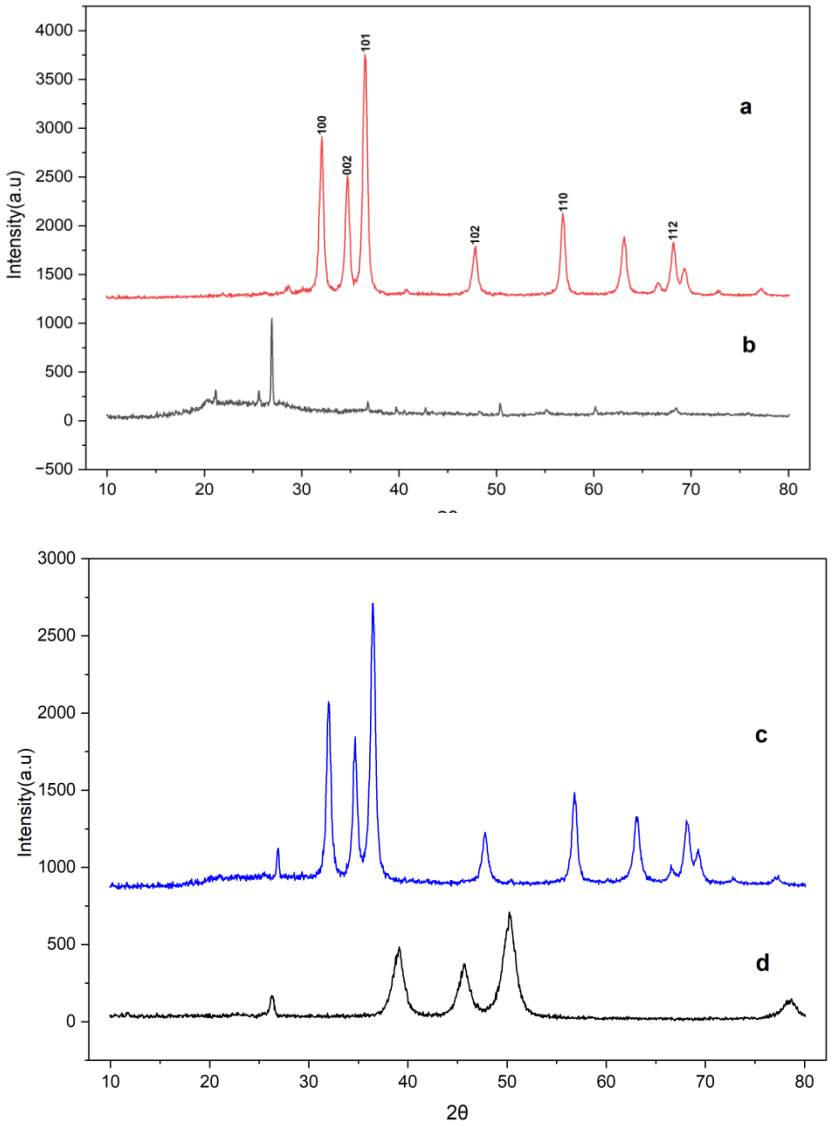

Fig.(3): The X-ray diffraction (XRD) patterns illustrate the structural characteristics of (a) ZnO-PP, (b) MK, (c) ZnO-MK prior to BF removal, and (d) ZnO-MK following BF removal.

3.1.3 Characterization of Functional Groups Using (FTIR) Spectroscopy

Fourier-Transform Infrared (FTIR) spectroscopy was employed to characterize the prepared materials, confirm chemical interactions, and verify the removal process. Fig (4) displays the FTIR spectra of four distinct samples: zinc oxide-modified potato peels (ZnO-PP), pure metakaolin (MK), the metakaolin-zinc oxide composite (ZnO-MK), and (ZnO-MK)after the removal of basic fuchsin. Fig (4-a) shows spectrum of zinc oxide-modified potato peels (ZnO-PP). The spectrum exhibited a strong and sharp absorption band at 417.5 cm^{-1},which is characteristically attributed to the stretching vibrations of the Zn-O bond. This confirms the successful loading of zinc oxide nanoparticles onto the surface of the potato peels. A broad band was also observed around 3420.1 cm^{-1}, corresponding to the O-H stretching vibrations of hydroxyl groups present in the cellulose and hemicellulose of the potato peels, as well as from surface-adsorbed water. Additionally, several peaks appeared in the fingerprint region. The sharp peaks at (1576.5, 1487.8, and 1378.8)cm^{-1} can be attributed to the bending vibrations of C-H bonds or the stretching vibrations of C=C and C=O bonds found in organic compounds like pectin and lignin within the potato peels.Alternatively, they might indicate the formation of carbonates on the surface due to the reaction of ZnO with atmospheric carbon dioxide. Furthermore, the peak observed at (1126.2 cm^{-1}) can be assigned to the C-O stretching vibrations in cellulose and hemicellulose. Moreover, Fig (4-b) shows spectrum of pure metakaolin (MK),The spectrum of pure metakaolin showed a prominent, very broad, and intense absorption band at 1076.0 cm^{-1}. This band represents the asymmetric stretching vibrations of Si-O-Al bonds, which is a distinctive signature of the silicate and aluminate framework of metakaolin. The other important band is observed at 470.5 cm^{-1}, representing the bending vibration of the O-Si-O bond. Thereafter, a shoulder peak at 798.8 cm^{-1} can be assigned to the symmetric stretching vibrations of the Si-O-Si network. A broad band also appears around 3428.4 cm^{-1} due to the O-H stretching vibration of surface-adsorbed water molecules. Finally, the weak peak at 2929.9 cm^{-1} can suggest the presence of small organic impurities possibly due to C-H stretching vibrations. Fig (4. -c) shows spectrum of the composite (ZnO-MK) before removal. In this spectrum, the characteristic bands of both metakaolin and zinc oxide were observed. The main absorption band of metakaolin appeared at 1054.8 cm^{-1}, showing a slight shift and a minor decrease in intensity compared to pure metakaolin. This suggests an interaction or bonding between the Si-O and Al-O groups on the metakaolin surface and the zinc oxide particles. The characteristic Zn-O band was also present at 432.9 cm^{-1}, confirming the successful formation of the composite as in Figure(4.1-e). The ZnO tensile vibration band appeared at 663.37$cm^{-1}$and the Al-OH vibration band at 910.40cm^{-1}, confirming the successful formation of the composite material. The absence of the main metakaolin (Si-O-Si/Si-O-Al) band was observed in the 1050cm^{-1}, indicating that the strong adsorption of the basic fuchsin dye led to a profound structural change or displacement in the surface bonding environment. This strong interaction explains the high efficiency of the material in adsorption of BF. The appearance of the basic fuchsin dye bands (C=C at 1504.47cm^{-1} and C-N at 1334.74cm^{-1}) indicates that the residues remaining after removal are strongly chemically bound to the active sites, making them resistant to the removal process. However, at the same time, it is evidence of the strong interaction nature of the material. The broad bands in the 3000-3900cm^{-1} region confirmed the presence of active O-H groups and adsorbed water molecules on the materials surface. These groups are crucial for the photocatalytic process, as they can react with photogenerated holes to produce highly reactive

(•OH). These radicals are powerful oxidizing agents that play a key role in the degradation of organic pollutants.

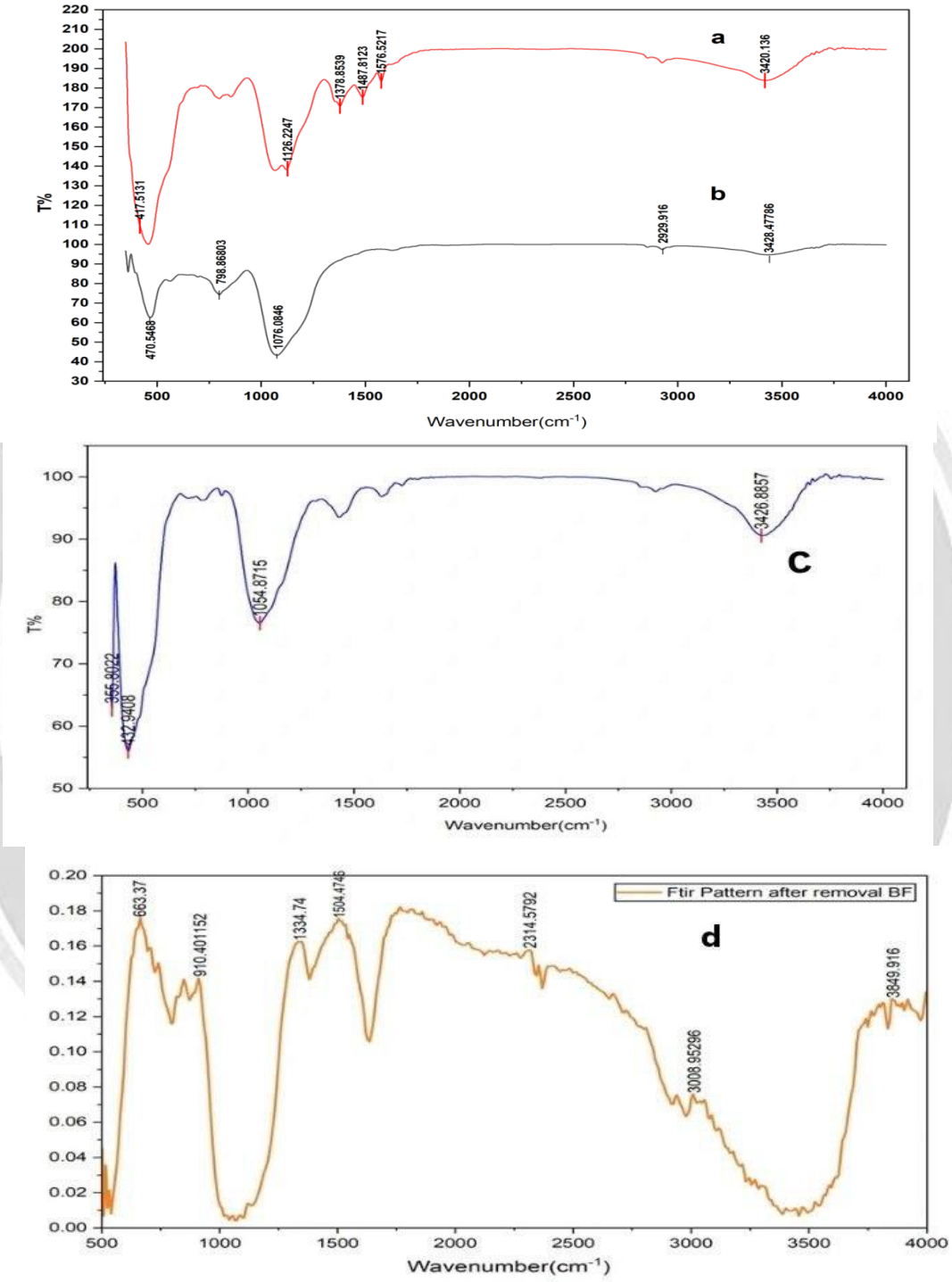

Fig.(4): FTIR spectra of (a) ZnO-PP, (b) MK ,(c) ZnO-MK before removal ,and (d) ZnO-MK after BF removal.

3.1.4 Morphological Analysis Using Field-Emission Scanning Electron Microscopy (FESEM):

To ascertain the morphology of the synthesized ZnO nanoparticles, a FESEM analysis of the ZnONPs was performed. For the FESEM investigations, FE-SEM was used to analyse the morphological characteristics and shape of the synthesis materials, as illustrated in fig.(5). The PP particles appear to have an irregular morphology. While some are observed as discrete particles, others appear clumped or grouped. Additionally, some particles are lamellar (like a sheet) while others are almost spherical. The substrate's surface, on which the particles rest, has voids and fissures and looks rough and uneven, as shown in fig.(5-a), this suggested that PP could be an excellent surface for ZnO nanoparticle synthesis. Fig.(5-b)shows the synthesized (ZnO-PP). It was found that the produced zinc oxide particles' sizes ranged from 44.73 nm, with some particles reaching the upper boundary of the nanoscals range. This distribution confirms the resultant particles' nanoscale nature, the surface area-to-volume ratio, which is essential for improving the material's physical and chemical properties, rises noticeably as a result of the small particle size in this range. The effectiveness of surface reactions is increased by the large surface area, which is a significant benefit in environmental and catalytic applications, such as Fig.(5-c).The metakaolin sample's FESEM pictures reveal a irregular morphology uneven surface structure and clusters of nanoparticles, these findings show a high surface area and porous structure appropriate for use in catalytic applications or nanocomposites, as well as the existence of quasi-spherical particles and notable nanoclustering. Fig (5-d) shows synthesis ZnO-MK with diameters ranging from roughly 35 to 57 nm, the nanoparticles have an irregular and clustered structure. The effective production of nanomaterials was indicated by the estimated average particle size of 46.66 nm. Because of their enormous surface area and nanoscale characteristics, their shape indicates that they may be suitable for photocatalytic or adsorption applications. Fig.(5-e) displays the ZnO-MK composite after being loaded with basic fuchsin dye, revealing nanoparticles that are non-uniformly distributed and exhibit significant with agglomerates, indicating good interaction between ZnO and metakaolin. The agglomerations are caused by the adsorption of dye molecules, confirming the activity of the composite in pollutant elimination. The porous and rough surface demonstrates a high active surface area, which is conducive to photocatalytic performance.

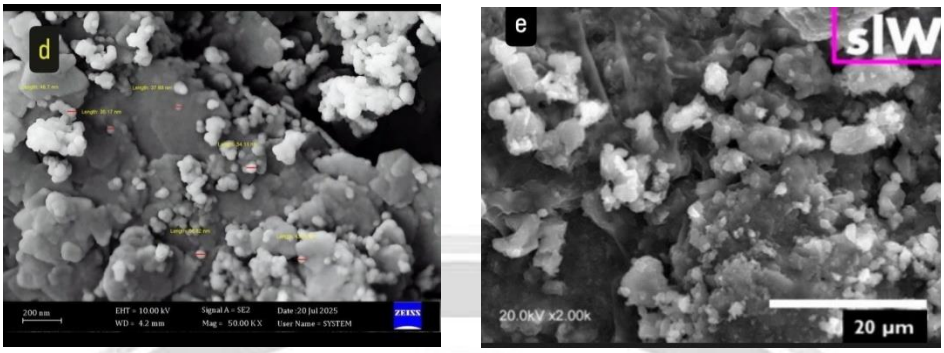

Fig.(5): FE-SEM micrographs of (a) PP, (b) ZnO-PP, (c) MK, and (d) ZnO-MK prior to BF removal, and (e) ZnO-MK following BF removal.

3.2 Batch Experiments:

3.2.1 Effect of pH:

The pH has both direct and indirect effects on the oxidation of organic compound. The advanced oxidation reactions are highly pH-dependent. The pH level affects hydroxyl radical formation and thus the oxidation efficiency [21]. The variations of pH value affect both the surface charge of the adsorbent and the degree of ionization, electrostatic interaction effects between the catalyst surface and functional groups separation at active sites of the catalyst, and solution chemistry. The description of the influences of pH on the efficiency of the photodegradation process is a very problematic task. This is because three reaction mechanisms may contribute to the degradation of dyes, (1) hydroxyl radical attack, (2) direct oxidation through the positive hole, and (3) direct reduction through the electron in the conducting band. The contribution of each one depends on the pH and substrate nature [22]. The effect of the different values of pH on the removal efficiency of BF was depicted in Fig.(6). As can be seen, the removal efficiency of BF was enhanced from 56% to 97% as the pH increased from 2 to 10. The results indicate that the ZnO-MK catalyst exhibited its maximum degradation performance at pH 7, achieving an efficiency of 97%.

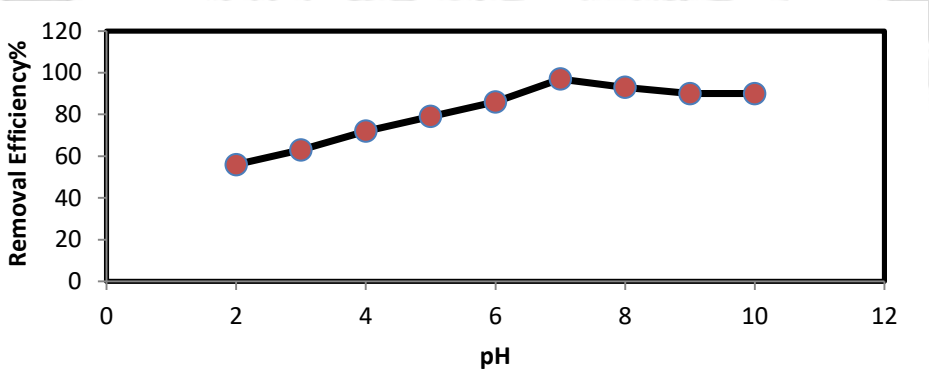

Fig.(6): Effect of pH on the degradation efficiency of (BF) under UV/ZnO-MK processes, (conc.=10ppm,t =120 min, and dose=0.2g/100ml).

3.2.2 Effect of dose:

The effect of catalyst loading on the photocatalytic degradation of acid fuchsin (BF) with the ZnO-MK composite was studied across a range of 0.025-0.25 g/100 mL Fig(7). The results showed that BF elimination effectiveness rose progressively with larger composite concentrations, peaking at 0.15 g/100 mL, which was determined as the best catalyst dose for this system. Beyond this concentration, up to 0.25 g/100 mL, the degradation rate followed a near-linear pattern, most likely due to competing interactions between composite particles in solution. At 0.15 g/100 mL, the number of accessible active sites on the composite surface and the production of hydroxyl radicals were maximized, resulting in improved BF elimination under UV irradiation. As a result, a catalyst loading of 0.15 g/100 mL was chosen for all future tests evaluating the photocatalytic performance of the ZnO-MK composite.

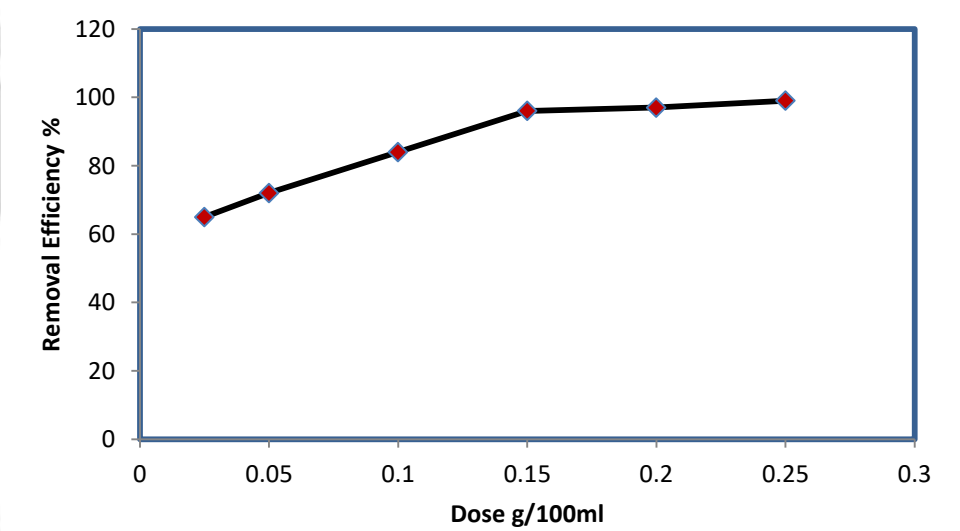

Fig. (7):Impact of dose on the degradation efficiency of (BF) under UV/ZnO–MK Processes, (conc.=10ppm, t=120mim, pH=7)

3.2.3 Effect of initial BF concentration:

The adsorbate uptake mechanism is particularly dependent on the initial concentration. At low concentrations, specific active sites adsorb contaminants, while at higher concentrations, a lower adsorption yield is due to the saturation of adsorption sites. Initial concentrations increased the number of collisions between adsorbate and sorbent, which could improve the adsorption process. On the other hand, the uptake increased with the increase in initial concentration, which caused an increase in the loading capacity of the sorbent, and this is due to the great driving force to overcome all mass transfer resistance between the adsorbent and aqueous media[23]. The results of the analysis on the influence of dye concentration are depicted in Fig.(8) following the determination of the optimal solution pH. To augment the breakdown of acid fuchsin by (ZnO-MK), an additional four doses of BF are required. The experimental findings presented in Fig. (8) indicate that increasing the initial concentration of acid fuchsin to 10 mg/L enhances the degradation efficiency. However, when the dye concentration exceeded 20 mg/L, the removal efficiency declined by more than 10%. This reduction is attributed to the influence of BF

molecules and intermediate degradation products on the photocatalytic process, including competitive adsorption of UV light [24]. Maximum degradation was achieved at 10 mg/L, where the ZnO-MK composite demonstrated optimal BF removal under the previously established ideal pH conditions [25].

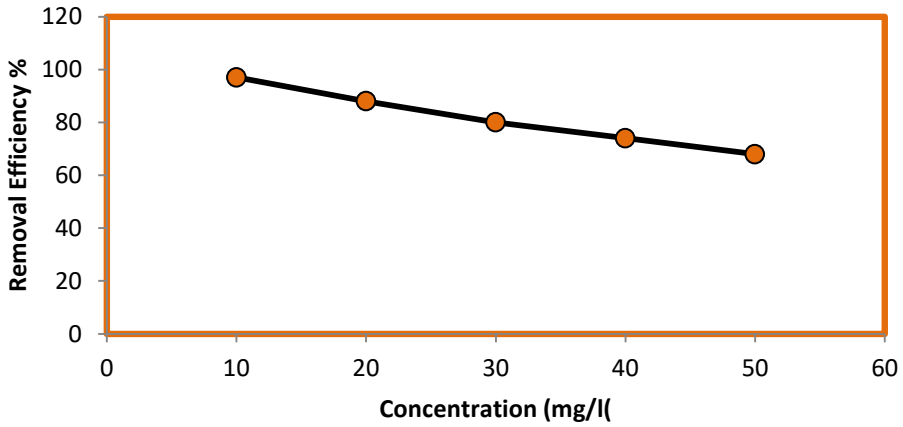

Fig.(8): Impact of Concentration on the degradation efficiency of (BF) under UV/ZnO–MK Processes, (Dose=0.15g/100ml, t=120mim, pH=7).

3.2.4 Effect of contact time:

The contact time was identified as a critical parameter influencing the efficiency of photocatalytic degradation. To establish the optimal reaction duration for the ZnO-MK catalyst, the percentage of basic fuchsin removal was monitored at different time intervals(Fig. 9). The results show that the degradation rate increased rapidly within the first 30 minutes and continued to rise progressively. Maximum removal efficiency was observed at approximately 120 minutes, after which the rate plateaued, remaining stable up to 180 minutes. Subsequently, it was noted that no additional degradation occurred. Consequently, the optimal duration for the elimination of basic fuchsin by the ZnO-MK composite, as indicated by the subsequent experiments, is 120 minutes [26].

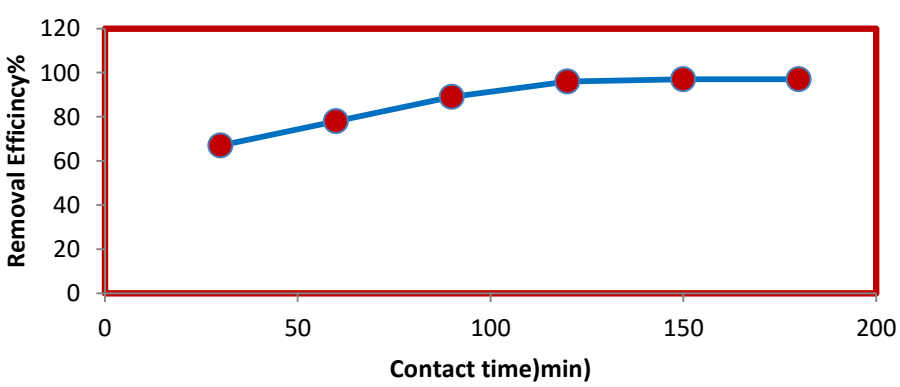

Fig. (9): Impact of Contact time on the degradation efficiency of (BF) under UV/ZnO–MK Processes, (Dose=0.15g/100ml, conc.=10ppm, pH=7).

3.3 Kinetic study:

The kinetics of photocatalytic degradation of basic fuchsin (BF) were investigated under the optimal parameters identified in the preceding experiments. Both pseudo-first-order (Eq.1) and pseudo-second-order(Eq.2) kinetic models were evaluated for a ZnO-MK dosage of 0.15 g/100 mL. As summarized in Table 3, the experimental data exhibited the closest agreement with the pseudo-first-order model, achieving a correlation coefficient of □² = 0.9526 (Figs. 10a and 10b). Accordingly, the kinetic behavior can be described by the following final model expression:

$$ln\frac{Co}{C} = K \qquad (1)$$

$$\frac{1}{C} - \frac{1}{Co} = Kt \qquad (2)$$

In this expression, □ denotes the reaction rate constant, while □₀ and □ correspond to the initial concentration and the concentration of BF at a given time (mg/L), respectively, and □ represents the elapsed reaction time in minutes.

Table 2: Reaction rate constants in heterogeneous photocatalysts.

pH=4,AF conc.=10ppm,ZnO-MK=0.2g/100ml			
First order		Second order	
K(min^{-1})	R^2	K(min^{-1})	R^2
0.0202	0.9526	0.0211	0.9264

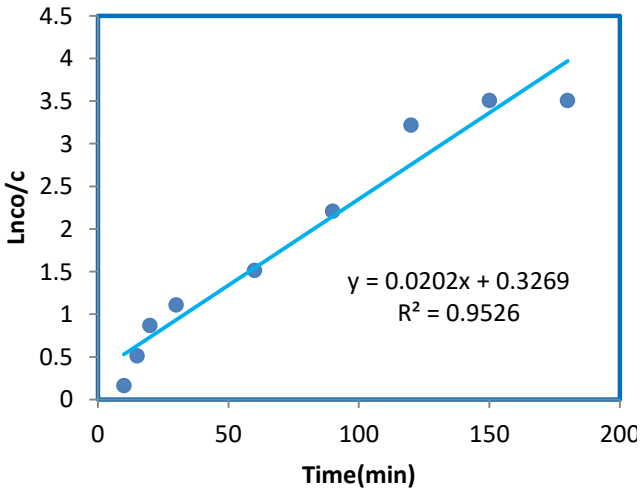

Fig. 10a. Kinetic analysis of BF degradation following the pseudo-first-order model under optimal conditions.

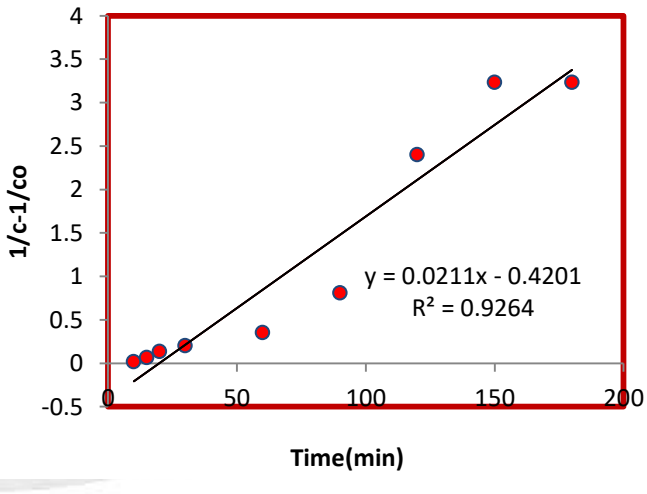

Fig. 10b. Kinetic analysis of BF degradation following the pseudo-second-order model under optimal conditions.

Conclusion:

A zinc oxide and metakaolin (ZnO-MK) composite was created, and ZnO was made from potato peel powder for green synthesis methods for removing basic fuchsin dye by photocatalytic method. Fourier transform infrared (FT-IR), X-ray diffraction (XRD), field-emission scanning electron microscopy (FE-SEM), energy dispersive spectroscopy (EDS), Brunauer–Emmett–Teller (BET), and Barrentt-Joyner-Halenda (BJH) were among the methods used to characterize ZnO-MK. The results indicated that 96% of the maximum removal efficiency was achieved at pH 7 and an initial BF concentration of 10 mg/L after 120 minutes. The green-synthesized ZnO-MK composite exhibited notable photocatalytic performance in the degradation of BF in aqueous solutions. These findings confirm the effectiveness of ZnO-MK as a catalyst in UV-driven photocatalytic processes for BF removal. Consequently, the ZnO-MK composite represents a cost-effective, environmentally friendly, and efficient semiconductor photocatalyst for the elimination of organic pollutants from water.

References

[1] O. Atolani, G.A. Olatunji, Chemical composition, antioxidant and cytotoxicity potential of Daniellia oliveri (Rolfe) Hutch. & Dalz, Turkish J. Pharm. Sci. 13 (2016) 41–46.

[2] M. Arulkumar, P. Sathishkumar, T. Palvannan, Optimization of Orange G dye adsorption by activated carbon of Thespesia populnea pods using response surface methodology, J. Hazard. Mater. 186 (2011) 827–834.

[3] B.K. Nandi, A. Goswami, M.K. Purkait, Adsorption characteristics of brilliant green dye on kaolin, J. Hazard. Mater. 161 (2009) 387–395.

[4] S. Imame, H. Atlas, J. Houssaini, M. Sadoq, M. Legsaier, K. Loukili, Removal and determination of basic fuchsin from wastewater using natural sugar cane bagasse by UV-Vis Spectrophotometry, 7 (2024) 33–50.

[5] K. Haroon, J. Kherb, C. Jeyaseelan, M. Sen, Recent Advances and Sustainable Approaches Towards Efficient Wastewater Treatment Using Natural Waste Derived Nanocomposites: A Review., Nat. Environ. Pollut. Technol. 22 (2023).

[6] E.N. Hidayah, O.H. Cahyonugroho, N.A. Fauziyah, Performance of Alum Coagulation and Adsorption on Removing Organic Matter and E. coli, Nat. Environ. Pollut. Technol. 22 (2023) 497–502.

[7] R.A. Al-Husseiny, S.E. Ebrahim, Synthesis of geopolymer for the removal of hazardous waste: A review, IOP Conf. Ser. Earth Environ. Sci. 779 (2021). https://doi.org/10.1088/1755-1315/779/1/012102.

[8] Z.H. Jabbar, B.H. Graimed, A.A. Okab, M.M. Alsunbuli, R.A. Al-husseiny, Construction of 3D flower-like Bi5O7I/Bi/Bi2WO6 heterostructure decorated NiFe2O4 nanoparticles for photocatalytic destruction of Levofloxacin in aqueous solution: Synergistic effect between S-scheme and SPR action, J. Photochem. Photobiol. A Chem. 441 (2023) 114734.

[9] M. Yu, Y. Ma, J. Liu, X. Li, S. Li, S. Liu, Sub-coherent growth of ZnO nanorod arrays on three-dimensional graphene framework as one-bulk high-performance photocatalyst, Appl. Surf. Sci. 390 (2016) 266–272.

[10] A. Roy, V. Singh, S. Sharma, D. Ali, A.K. Azad, G. Kumar, T. Bin Emran, Antibacterial and dye degradation activity of green synthesized iron nanoparticles, J. Nanomater. 2022 (2022) 3636481.

[11] M. Riaz, M. Zia-Ul-Haq, B. Saad, Anthocyanins and human health: biomolecular and therapeutic aspects, Springer, 2016.

[12] A. Awwad, A. M., University of California Santa Cruz (Organization), T. Boldoo, J. Ham, E. Kim, H. Cho, S.K. Chandraker, M.K. Ghosh, M. Lal, R. Shukla, J. Singh, T. Dutta, K.H. Kim, M. Rawat, P. Samddar, P. Kumar, A. Singh, P.K. Gautam, A. Verma, V. Singh, P.M. Shivapriya, S. Shivalkar, A.K. Sahoo, S.K. Samanta, Infrared Tables, Nano Express 13 (2020) e00427. https://doi.org/10.1016/j.btre.2020.e00427%0Ahttps://doi.org/10.1186/s12951-018-0408-4.

[13] S. Modi, V.K. Yadav, D. Ali, N. Choudhary, S. Alarifi, D.K. Sahoo, A. Patel, M.H. Fulekar, Photocatalytic Degradation of Methylene Blue from Aqueous Solutions by Using Nano-ZnO/Kaolin-Clay-Based Nanocomposite, Water (Switzerland) 15 (2023). https://doi.org/10.3390/w15223915.

[14] V.K.Y. 1 Nisha Choudhary 1,*, Remediation_of_Methylene_Blue_Dye_from_W.pdf, (2023).

[15] S.Z. Run Zhao, Investigating the Electrocatalytic properties of ZnO-Based composite membrane for dye removal, (2025).

[16] R. Noroozi, T.J. Al-Musawi, H. Kazemian, E.M. Kalhori, M. Zarrabi, Removal of cyanide using surface-modified Linde Type-A zeolite nanoparticles as an efficient and eco-friendly material, J. Water Process Eng. 21 (2018) 44–51.

[17] X. Wei, G. Zhu, J. Fang, J. Chen, Synthesis, Characterization, and Photocatalysis of Well-Dispersible Phase-Pure Anatase TiO2 Nanoparticles, Int. J. Photoenergy 2013 (2013) 726872.

[18] V. Selvanathan, M. Aminuzzaman, L.X. Tan, Y.F. Win, E.S.G. Cheah, M.H. Heng, L.-H. Tey, S. Arullappan, N. Algethami, S.S. Alharthi, Synthesis, characterization, and preliminary in vitro antibacterial evaluation of ZnO nanoparticles derived from soursop (Annona muricata L.) leaf extract as a green reducing agent, J. Mater. Res. Technol. 20 (2022) 2931–2941.

[19] K. Weise, N. Ukrainczyk, A. Duncan, E. Koenders, Enhanced metakaolin reactivity in blended cement with additional calcium hydroxide, Materials (Basel). 15 (2022) 367.

[20] S. Drummer, T. Madzimbamuto, M. Chowdhury, Green synthesis of transition-metal nanoparticles and their oxides: A review, Materials (Basel). 14 (2021). https://doi.org/10.3390/ma14112700.

[21] X.-K. Zhao, G.-P. Yang, Y.-J. Wang, X.-C. Gao, Photochemical degradation of dimethyl phthalate by Fenton reagent, J. Photochem. Photobiol. A Chem. 161 (2004) 215–220.

[22] K.M.R.• A.K.• F. Gulshan2, Parameters affecting the photocatalytic degradation of dyes using TiO2: a review, (2017).

[23] Green Synthesis of ZnO Nano-composite Using Onion Peels Extract for Photocatalytic Removal of Cefixime and Tetracycline A, (2025).

[24] M. Falah, K.J.D. Mackenzie, Photocatalytic nanocomposite materials based on inorganic polymers (Geopolymers): A review, Catalysts 10 (2020) 1–20. https://doi.org/10.3390/catal10101158.

[25] F.A. Alharthi, N. Al-Zaqri, A. El Marghany, A.A. Alghamdi, A.Q. Alorabi, N. Baghdadi, H.S. Al-Shehri, R. Wahab, N. Ahmad, Synthesis of nanocauliflower ZnO photocatalyst by potato waste and its photocatalytic efficiency against dye, J. Mater. Sci. Mater. Electron. 31 (2020) 11538–11547.

[26] J. Liu, S. Wei, H. Zhang, Y. Deng, J. Baeyens, R. Dewil, N. Sweygers, L. Appels, Adsorption of acid fuchsine dye from wastewater by Mg-ferrite particles, J. Environ. Manage. 317 (2022) 115427.

ARTICLE
JOURNAL`S UNIVERSITY OF BABYLON FOR ENGINEERING SCIENCES (JUBES)
مـــجلـة جـــامعة بـــابـل للعلـــوم الهندسية
Vol. 33, No.6. \ 2025 ISSN: 2616 - 9916

التحلل الضوئي الحفزي للفوكسين القاعدي من المحاليل المائية باستخدام مركب أكسيد الزنك / ميتاكاولين

ابتهاج احمد رحيم الاعرجي **رشا علي طه الحسيني**

قسم هندسة إدارة الموارد المائية، كلية الهندسة، جامعة القاسم الخضراء

ebtehijahmed@wrec.uoqasim.edu.iq rasha83@wrec.uoqasim.edu.iq

الخلاصة:-

تُعدّ الملوثات العضوية الخطرة مشكلة بيئية شائعة، إذ لا تتحلل بسهولة في البيئة، مما يؤدي إلى تراكمها وتأثيرها السلبي على النظم البيئية وصحة الإنسان. لذلك، يُعدّ إيجاد طرق فعّالة ومستدامة للتخلص منها أمرًا بالغ الأهمية للحفاظ على البيئة والحد من المخاطر الصحية المرتبطة بها. ونتيجةً لذلك، قدّم هذا العمل تقنيةً فعّالة من حيث التكلفة وصديقة للبيئة ومباشرة لتحضير مادة نانوية مركبة من أكسيد الزنك باستخدام قشور البطاطا(PP)هذه المادة النانوية المركبة، المعروفة باسم (ZnO–PP)، تم دمجها لاحقًا مع الميتاكاولين لتكوين مادة مركبة مصممة لتسهيل عملية الأكسدة المتقدمة(AOP) لإزالة صبغة الفوكسين القاعدية (BF) من الأوساط المائية .تم إجراء توصيف شامل للمواد المركبة المحضّرة باستخدام عدة أدوات تحليلية، بما في ذلك مطيافية الأشعة تحت الحمراء بتحويل فوريه(FTIR) ، وحيود الأشعة السينية (XRD)، والمجهر الإلكتروني الماسح ذي الانبعاث المجالي(FESEM) ، وتحليل مساحة السطح النوعية(BET) . أشارت نتائج إلى أن مساحة السطح النوعية تبلغ 2.95 م²/غ لقشور البطاطس الخام(PP) ، و 15.985 م²/غ لمادة(ZnO–PP) ، و 28.251 م²/غ لمادة المركبة(ZnO–MK).تحت الظروف المثلى، والتي شملت جرعة 0.15 غرام من مركب لكل 100 مل من المحلول، وتركيزًا أوليًا لصبغة(BF) يبلغ 10 ملغم/لتر، وزمن تلامس قدره 120 دقيقة، ودرجة حموضة (pH) تساوي 7، حققت المادة المركبة أقصى كفاءة لإزالة الصبغة بنسبة 96%. وكشف التقييم الحركي أن تحلل صبغة يتوافق مع نموذج معدل الرتبة الأولى الكاذبة ، مع معامل تحديد(R^2) قدره 0.9526

الكلمات الدالة:- فوكسين قاعدي (BF), التصنيع الاخضر , تحلل ضوئي حفزي, قشور بطاطا(PP) , أكسيد الزنك(ZnO).